



Heavy quarkonium in $p\text{Pb}$ collisions and fixed-target results at LHCb

Jiayin Sun
Tsinghua University

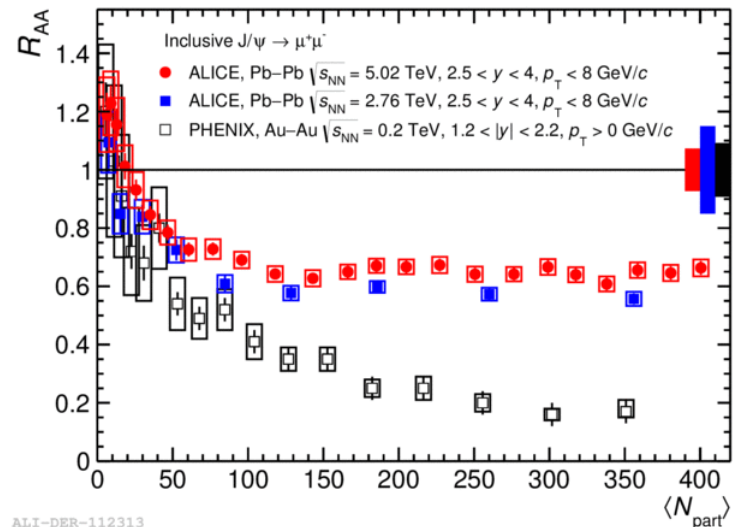
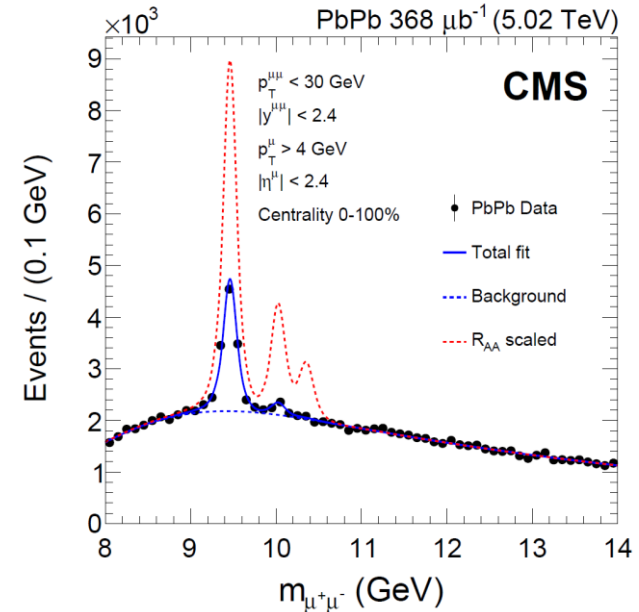
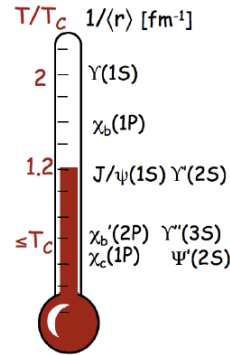
The 2nd FCPPL quarkonium production workshop

Outline

- Quarkonium in $p\text{Pb}$
 - J/ψ
 - Upsilon $\Upsilon(nS)$
- Fixed target results
 - Charm production cross-section
 - Antiproton production cross-section

Quarkonia in PbPb Collisions

- Color screening: $Q\bar{Q}$ potential is screened by surrounding color charge, leading to dissociation
 - J/ψ suppression a signature of deconfinement
- Sequential melting: quarkonia states (e.g. Υ family) dissociate at different temperatures
 - QGP thermometer
- Hot medium effects:
 - Suppression by color screening
 - Regeneration via statistical recombination
 - Medium induced energy loss
- Cold nuclear matter (CNM) effects
 - Studied via proton-nucleus collisions
 - Crucial for the interpretation of AA results

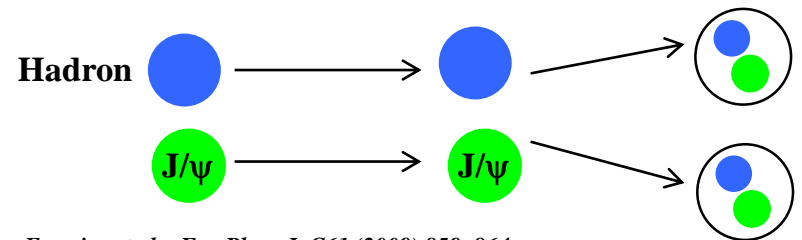
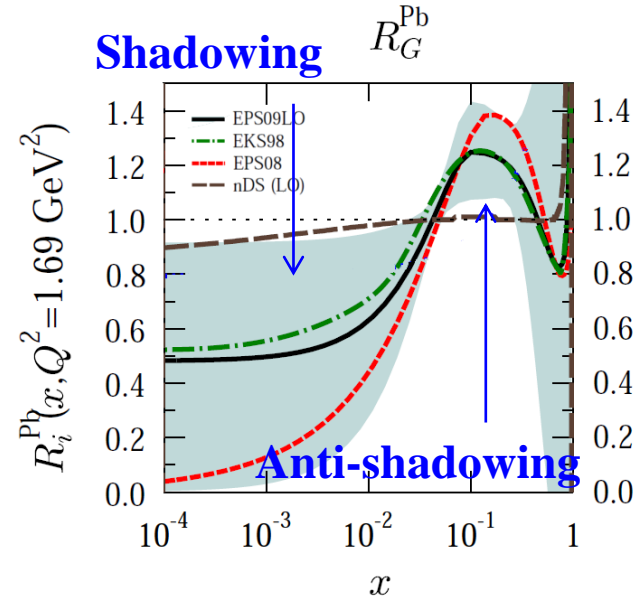


ALI-DER-112313

Quarkonia in $p\text{Pb}$ Collisions

Ferreiro et al., PRC 81(2010) 064911
Eskola et al., Eur.Phys.J. C9 (1999) 61-68
Eskola. et al., JHEP 0807 (2008) 102
Eskola et al., JHEP 0904 (2009) 065
De Florian et al., PRD69 (2004) 074028

- Cold Nuclear Matter effects
 - Initial state:
 - Modification of nuclear PDF
 - Gluon saturation
 - Multiple scattering of partons in the nucleus
 - Final state:
 - nuclear absorption (negligible at LHC energy)
 - Co-movers effect
 - Break-up of quarkonium by co-moving hadrons outside of nuclear remnant
 - study via $\psi(2S)$, $\Upsilon(nS)$
 -

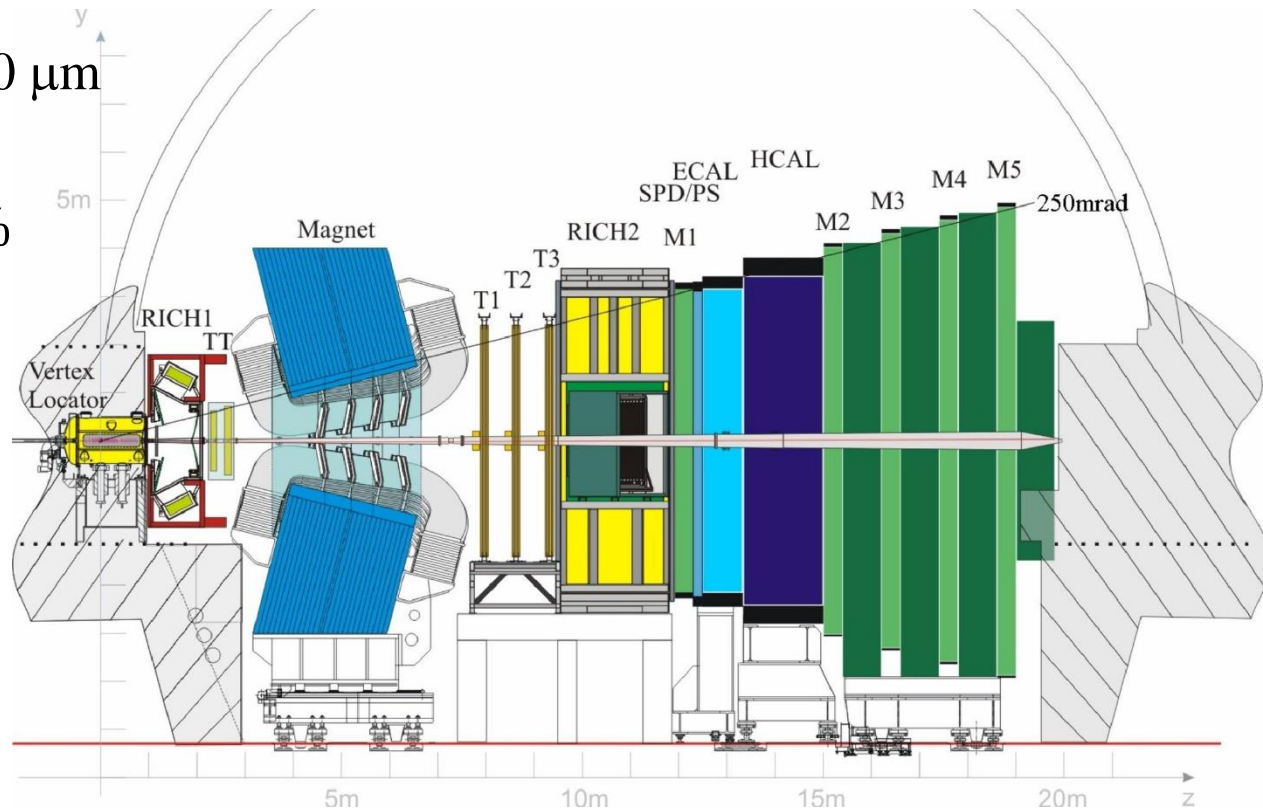


Ferreiro et al., Eur.Phys. J. C61 (2009) 859-864
Ferreiro et al., PLB680 (2009) 50-55
Ferreiro, et al., PRC81 (2010) 064911

Co-mover effect

LHCb detector

- A single arm forward spectrometer designed for the study of particles containing c or b quark.
- Acceptance: $2 < \eta < 5$
- Vertex detector
 - IP resolution $\sim 20 \mu\text{m}$
- Tracking system
 - $\frac{\Delta p}{p} = 0.5\% - 1\%$
(5-200 GeV/c)
- RICH
 - K/ π /p separation
- Electromagnetic
+ hadronic
Calorimeters
- Muon systems

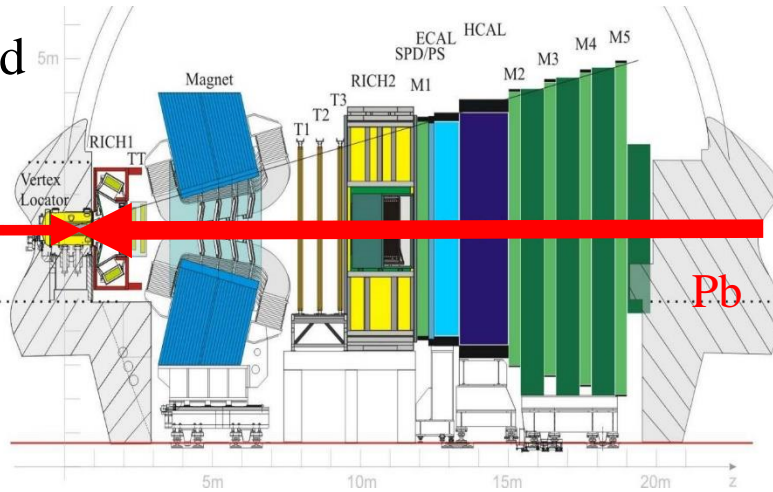


$p\text{Pb}$ @ 8 TeV dataset

Forward

$p\text{Pb}$

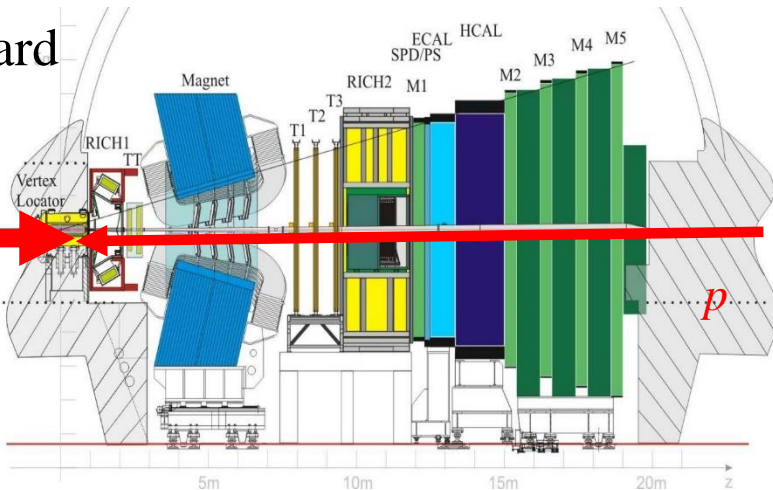
p



Backward

$\text{Pb}p$

Pb



- Rapidity Coverage

- y^* : rapidity in nucleon-nucleon cms
- $y_{\text{cms}} = \pm 0.465$
- Forward: $1.5 < y^* < 4.0$
- Backward: $-5.0 < y^* < -2.5$
- Common region: $2.5 < |y^*| < 4.0$

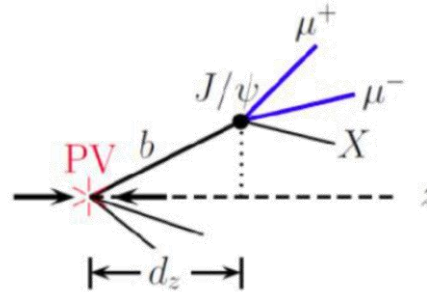
- $\sqrt{s_{NN}} = 8 \text{ TeV}$ (2016)

- $p\text{Pb}$ (13.6 nb^{-1}) + $\text{Pb}p$ (21.8 nb^{-1})

Prompt and nonprompt J/ψ in $p\text{Pb}$ at 8 TeV

- Sources

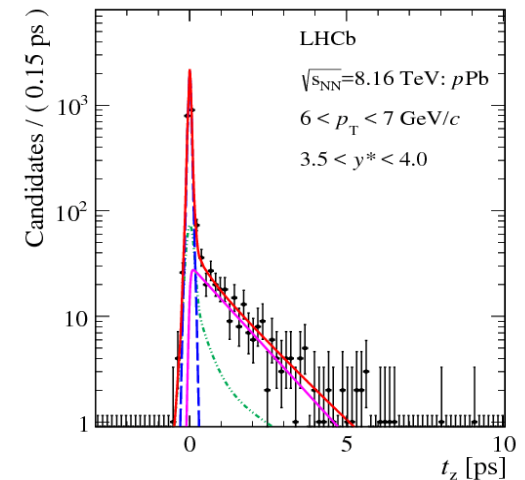
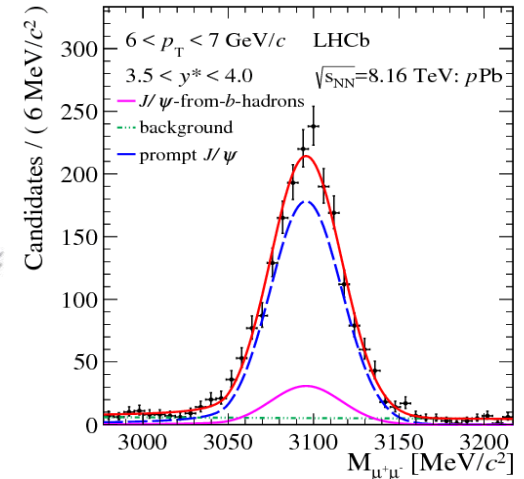
- Prompt: direct production, feed down from heavier states $\psi(2S)$, χ_c
- Nonprompt: from b -hadrons decays



- First Run2 result in heavy ion collisions
- Reconstructed through $J/\psi \rightarrow \mu^+ \mu^-$
- Prompt and nonprompt (from b -hadrons) separated: the pseudo proper decay time

$$t_z \equiv \frac{(z_{J/\psi} - z_{PV}) \times M_{J/\psi}}{p_z}$$

- Signal extraction with 2D simultaneous fit to mass and the pseudo proper decay time



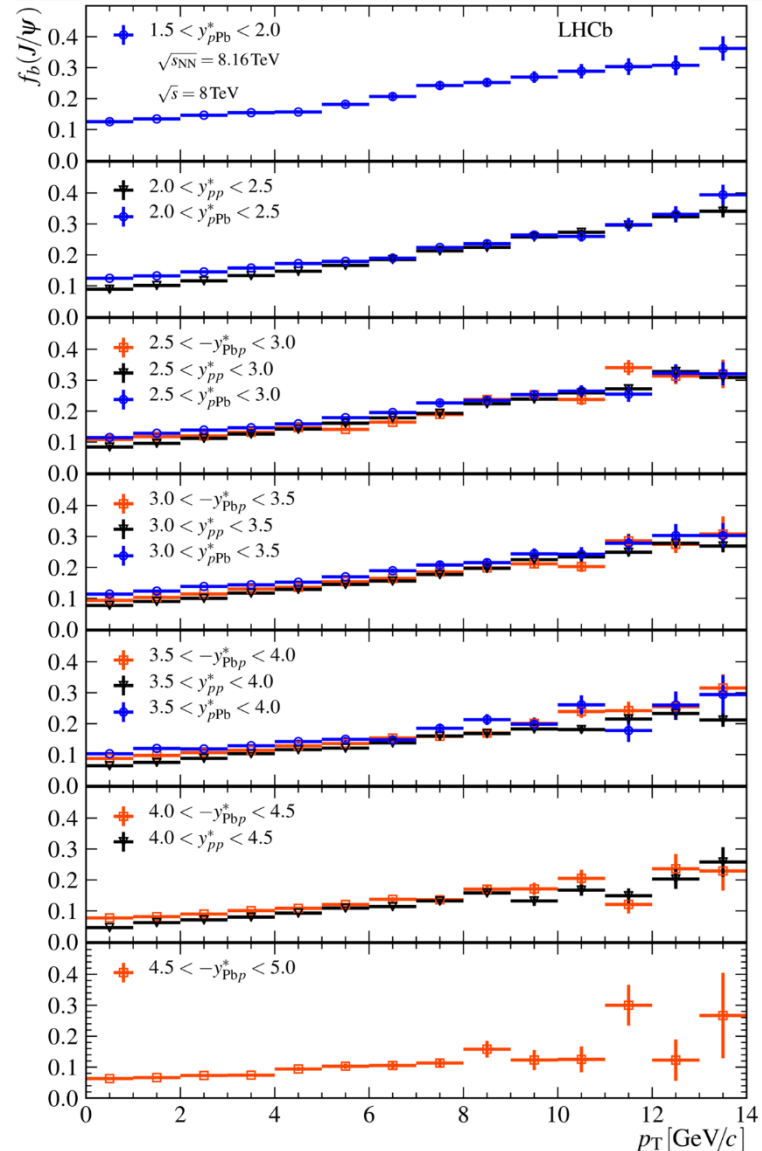
Prompt and nonprompt J/ψ in p Pb at 8 TeV

- Separation of prompt and nonprompt J/ψ with p_T down to 0

- Fraction from b hadrons:

$$f_b = \frac{\frac{d^2\sigma_{J/\psi\text{-from-}b}}{dp_T dy^*}}{\frac{d^2\sigma_{\text{Prompt } J/\psi}}{dp_T dy^*} + \frac{d^2\sigma_{J/\psi\text{-from-}b}}{dp_T dy^*}}$$

- pp , forward, backward compared:
 - similar trends
 - Increasing with p_T
 - Small differences at low p_T : cold nuclear matter effects different for the prompt and nonprompt

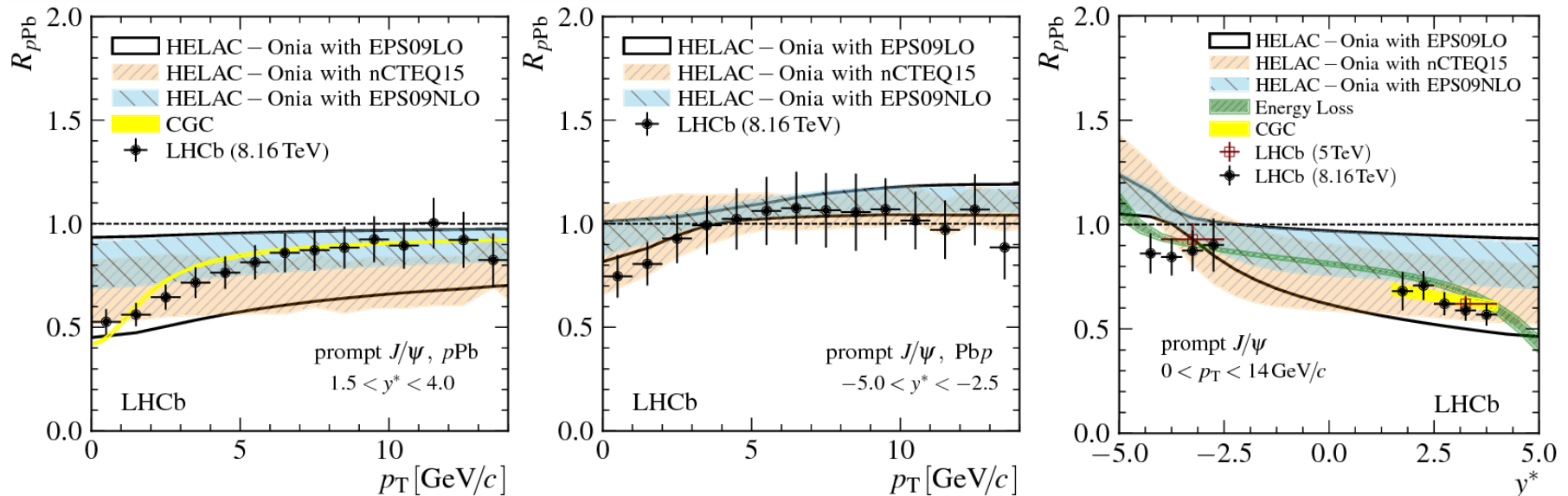


Prompt J/ψ at 8 TeV

nuclear modification factor in $p\text{Pb}$

$$R_{p\text{Pb}}(y^*, p_T) = \frac{1}{A} \times \frac{d\sigma_{p\text{Pb}}(y^*, p_T, \sqrt{s_{NN}})/dx}{d\sigma_{pp}(y^*, p_T, \sqrt{s_{NN}})/dx}, \quad A=208$$

- **pp reference:** interpolation of LHCb measurements at 7, 8 and 13 TeV
- **Forward rapidity:** suppression up to 50% at low p_T , decreasing with increasing p_T
- **Backward rapidity:** closer to unity
- Overall agreement with models with large uncertainties on the gluon PDFs at low x
- Compatible with 5 TeV results

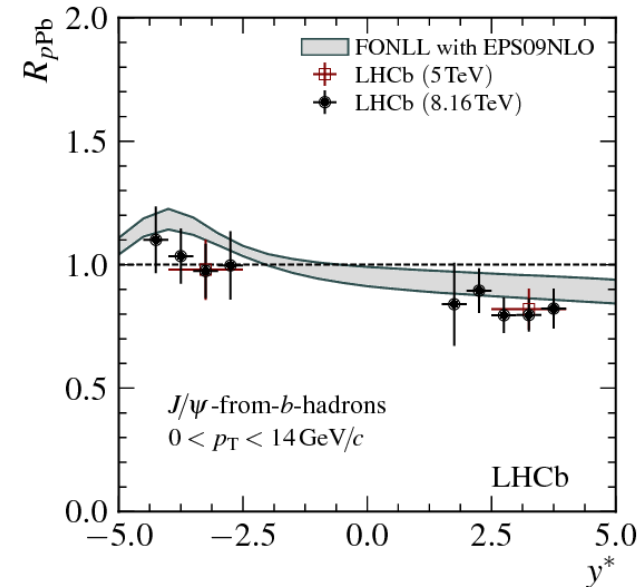
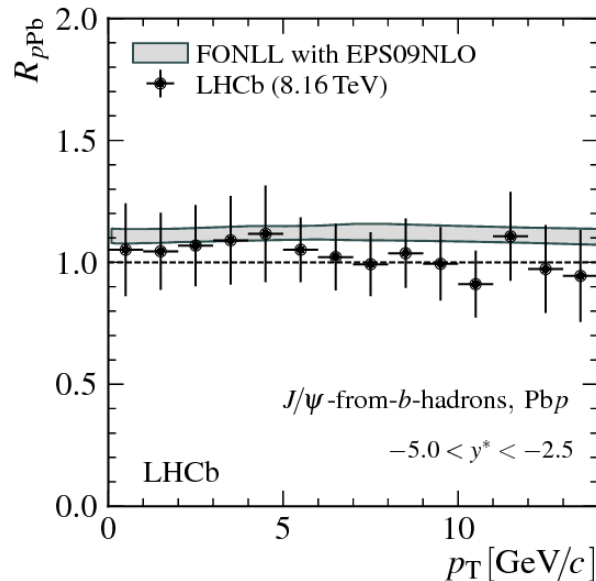
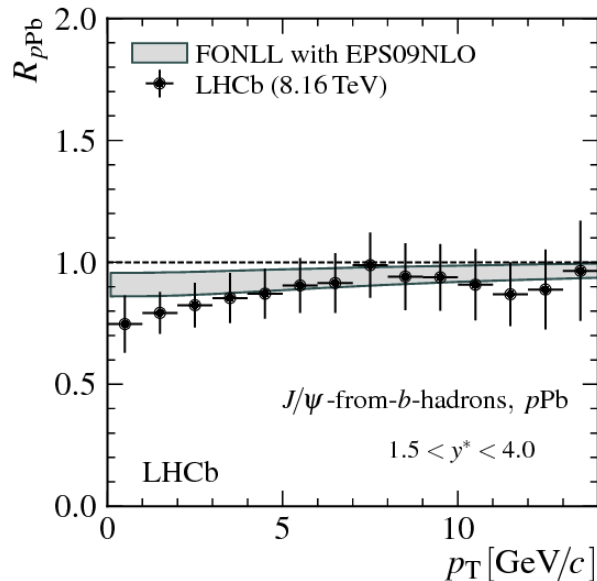


J/ψ -from- b -hadrons at 8 TeV nuclear modification factor in $p\text{Pb}$

$$R_{p\text{Pb}}(y^*, p_T) = \frac{1}{A} \times \frac{d\sigma_{p\text{Pb}}(y^*, p_T, \sqrt{s_{NN}})/dx}{d\sigma_{pp}(y^*, p_T, \sqrt{s_{NN}})/dx}, \quad A=208$$

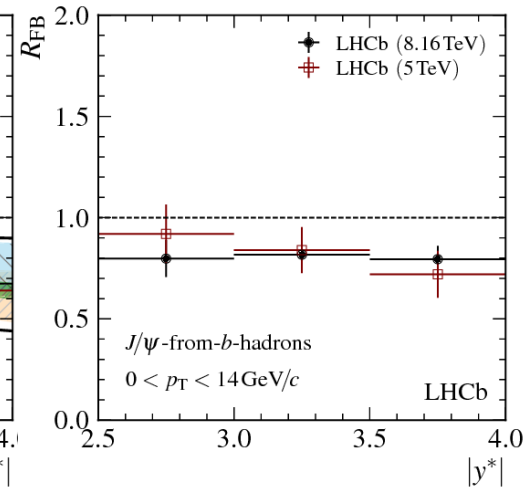
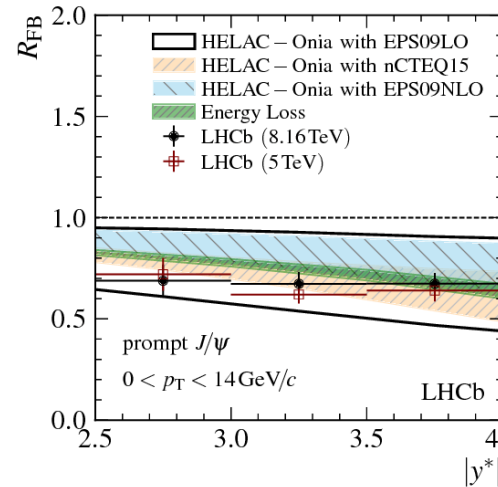
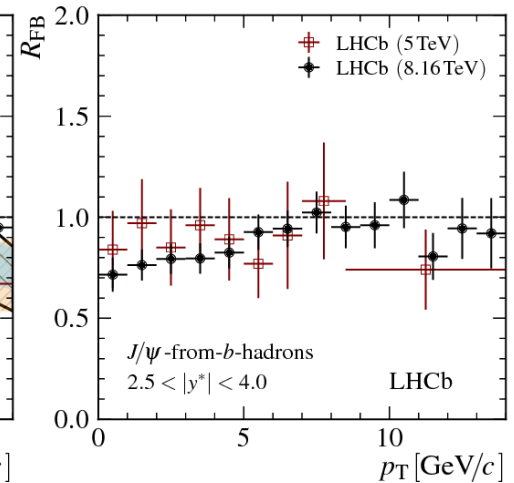
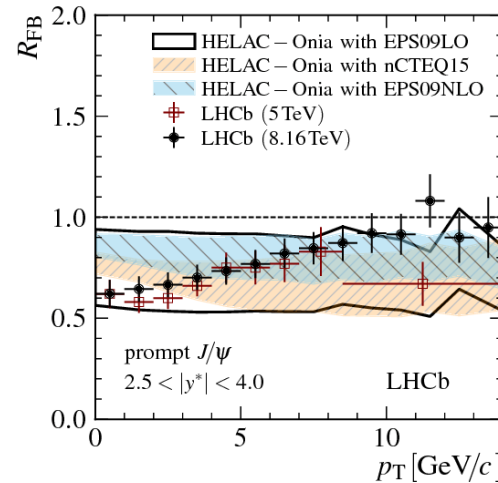
- **pp reference:** interpolation of LHCb measurements at 7, 8 and 13 TeV
- **Forward rapidity:** smaller suppression up to 30% at low p_T , reach unity at higher p_T
- **Backward:** compatible with unity
- FONLL with EPS09NLO consistent with data
- Compatible with 5 TeV results

EPS09 JHEP 04 (2009) 065



Prompt J/ψ at 8 TeV forward-backward production ratio

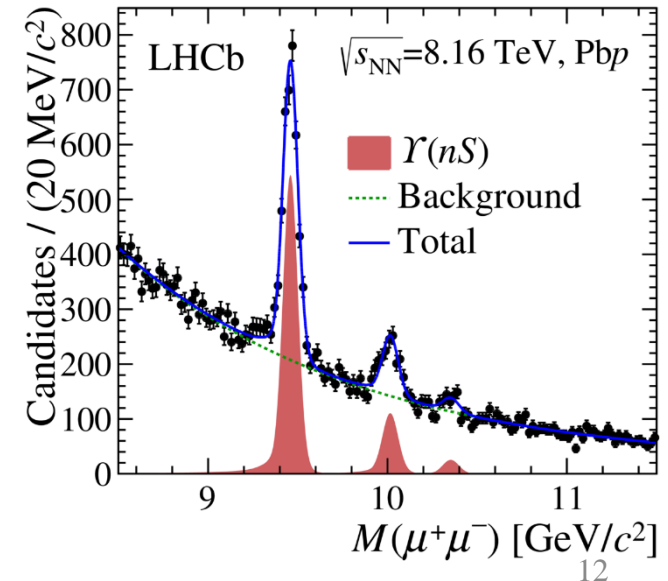
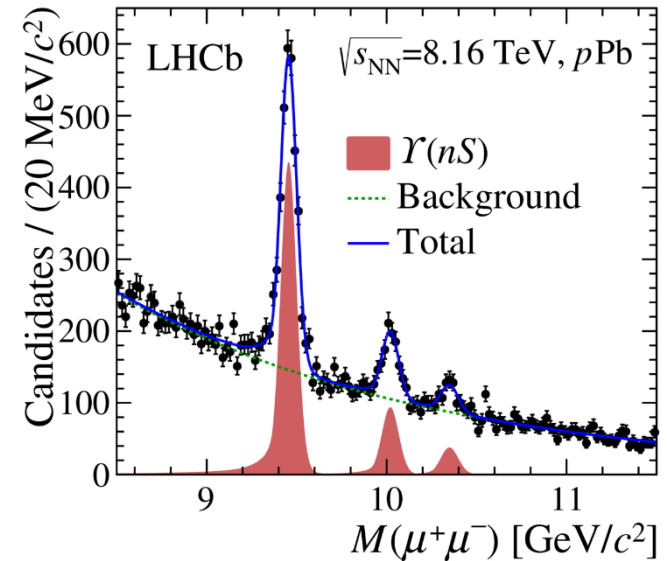
- $R_{FB} = \frac{d\sigma(+|y^*|, p_T)/dx}{d\sigma(-|y^*|, p_T)/dx}$
- R_{FB} does not need inputs from pp collisions.
- Prompt J/ψ :
 - Clear forward-backward asymmetry
 - Increasing trend with increasing p_T
- Nonprompt J/ψ :
 - Closer to unity
- Models for prompt J/ψ only
- Consistent with 5 TeV results



$\Upsilon(nS)$ in $p\text{Pb}$ collisions

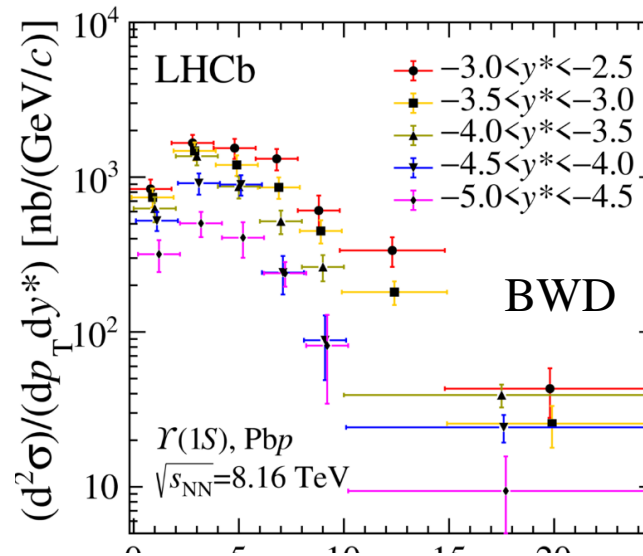
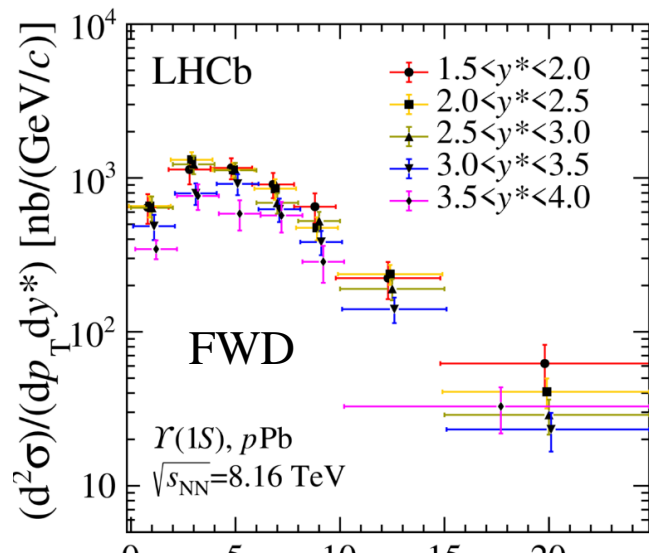
JHEP 11 (2018) 194

- New differential analysis of 2016 $p\text{Pb}$ data
 - Double differential for $\Upsilon(1S)$
 - Single differential for $\Upsilon(2S)$
- Cross-section, $R_{p\text{Pb}}$, double ratio of $\Upsilon(nS)/\Upsilon(1S)$ for all $\Upsilon(nS)$ states
- Nice $\Upsilon(3S)$ signals in forward and backward configurations

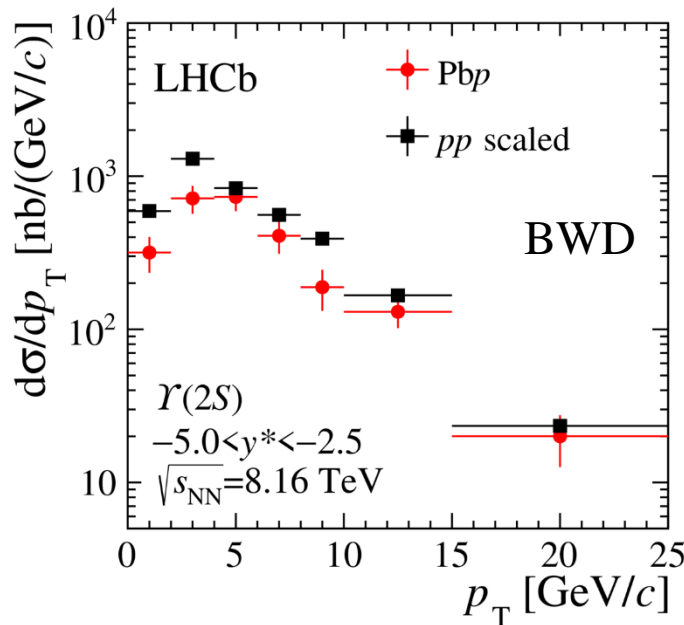
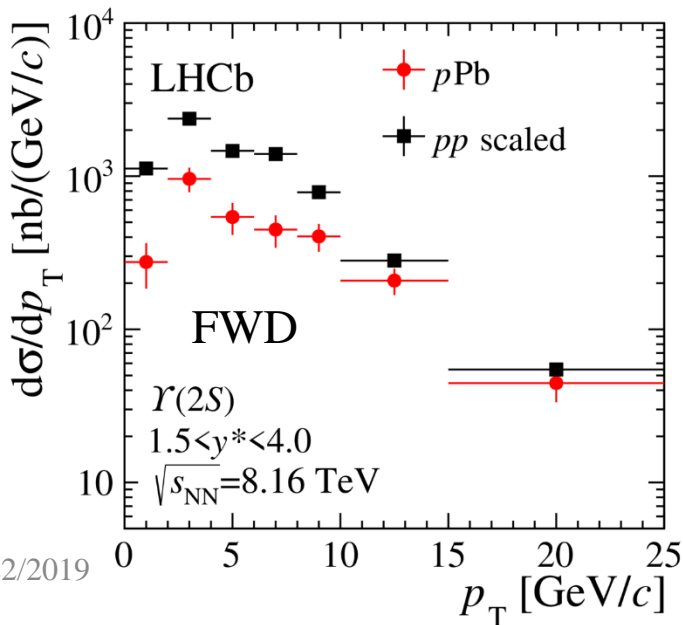


Samples	$\Upsilon(1S)$	$\Upsilon(2S)$	$\Upsilon(3S)$	\mathcal{L}
$p\text{Pb}$	2705 ± 87	584 ± 49	262 ± 44	12.5 nb^{-1}
PbP	3072 ± 82	679 ± 54	159 ± 39	19.3 nb^{-1}

$\Upsilon(nS)$ cross-section



$\leftarrow \Upsilon(1S)$



$\leftarrow \Upsilon(2S)$

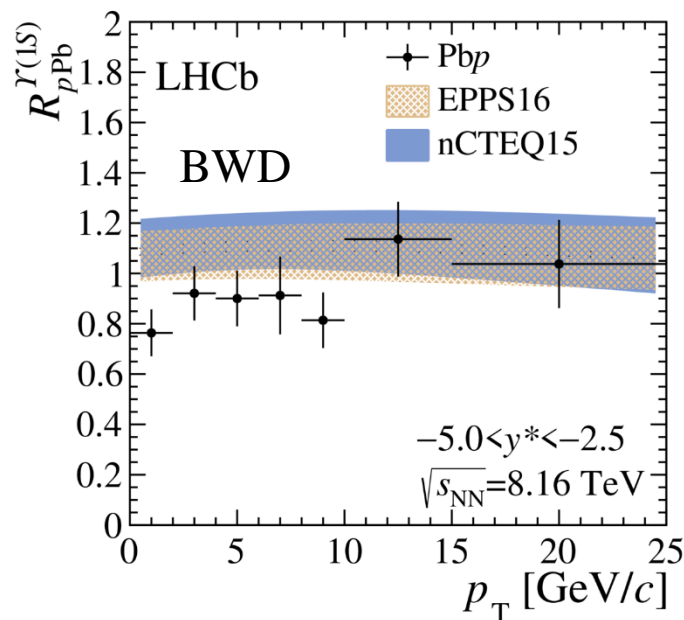
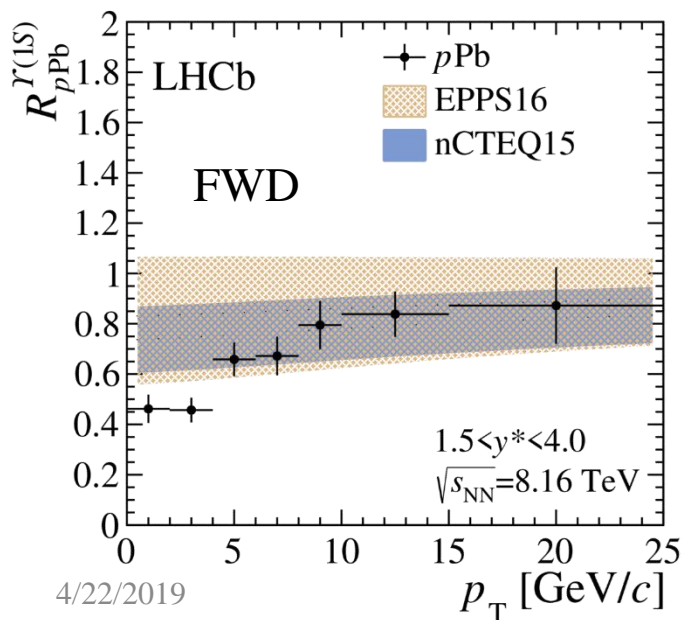
$\Upsilon(1S)$ nuclear modification factor

$$R_{pPb}(y^*, p_T) = \frac{1}{A} \times \frac{d\sigma_{pPb}(y^*, p_T, \sqrt{s_{NN}})/dx}{d\sigma_{pp}(y^*, p_T, \sqrt{s_{NN}})/dx}, \quad A=208$$

pp reference: interpolation of LHCb measurements at 2.76, 7, 8 and 13 TeV

Forward rapidity: suppression for $\Upsilon(1S)$ and $\Upsilon(2S)$ states, compatible with nPDFs

Backward rapidity: $\Upsilon(2S)$ more suppressed than $\Upsilon(1S)$, consistent with nPDFs+comovers calculation



$\Upsilon(1S)$

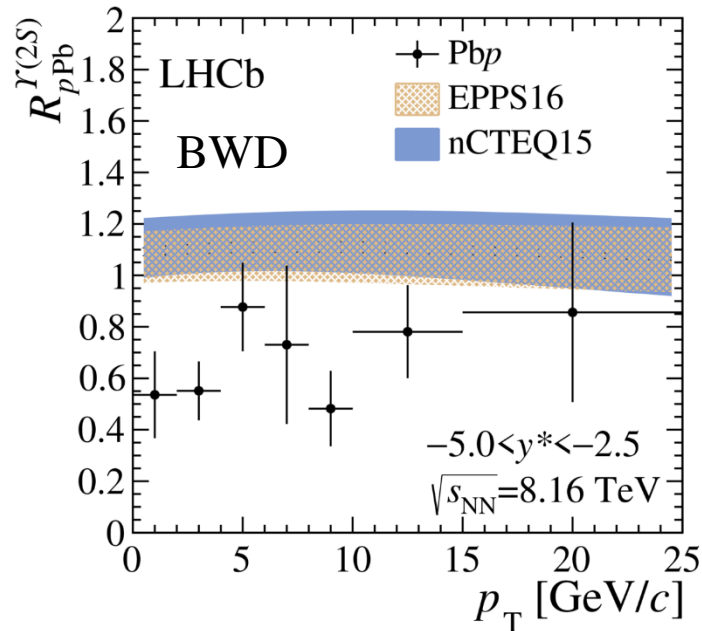
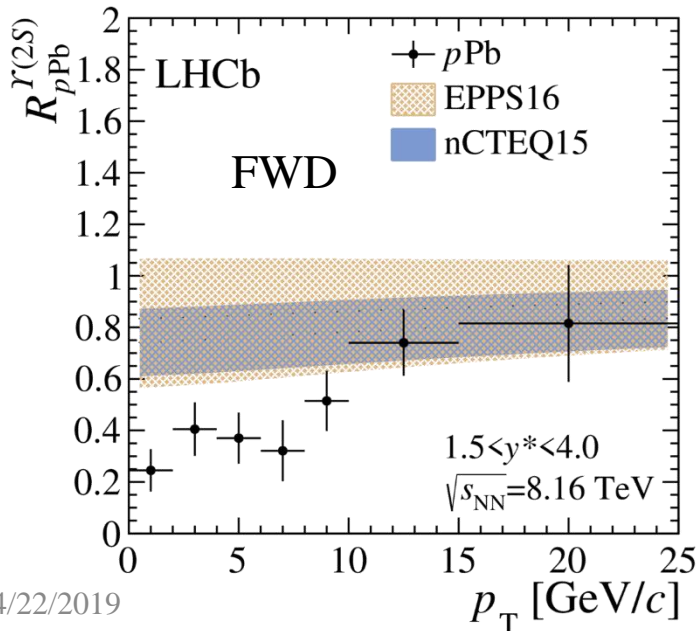
$\Upsilon(2S)$ nuclear modification factor

$$R_{pPb}(y^*, p_T) = \frac{1}{A} \times \frac{d\sigma_{pPb}(y^*, p_T, \sqrt{s_{NN}})/dx}{d\sigma_{pp}(y^*, p_T, \sqrt{s_{NN}})/dx}, \quad A=208$$

pp reference: interpolation of LHCb measurements at 2.76, 7, 8 and 13 TeV

Forward rapidity: suppression for $\Upsilon(1S)$ and $\Upsilon(2S)$ states, compatible with nPDFs

Backward rapidity: $\Upsilon(2S)$ more suppressed than $\Upsilon(1S)$, consistent with nPDFs+comovers calculation



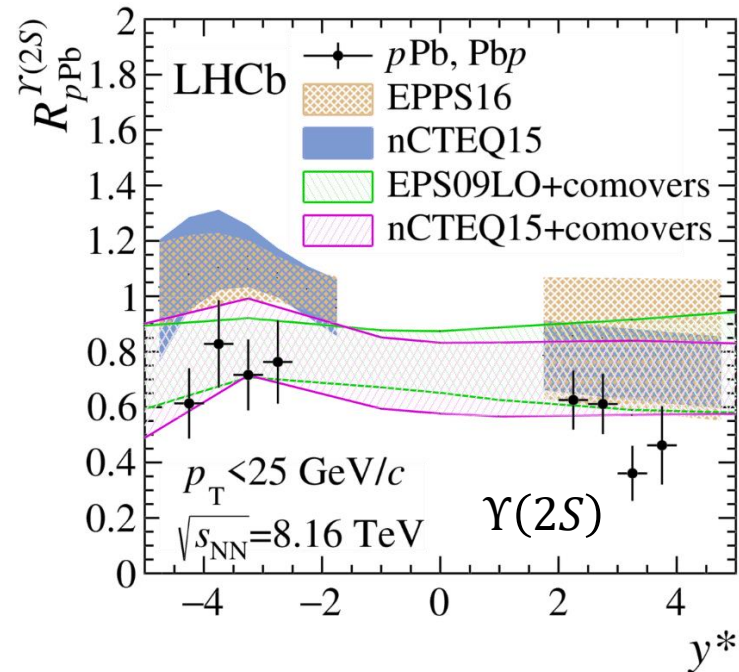
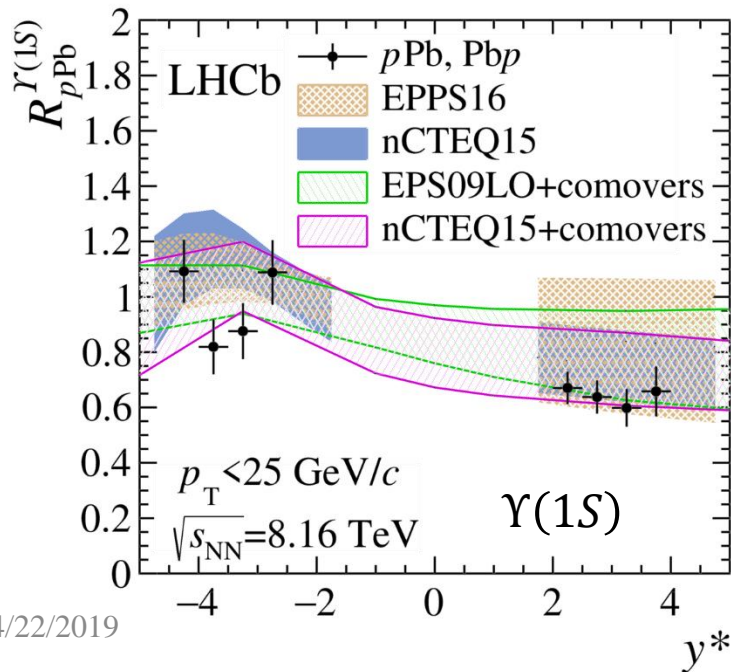
$\Upsilon(nS)$ nuclear modification factor

$$R_{pPb}(y^*, p_T) = \frac{1}{A} \times \frac{d\sigma_{pPb}(y^*, p_T, \sqrt{s_{NN}})/dx}{d\sigma_{pp}(y^*, p_T, \sqrt{s_{NN}})/dx}, \quad A=208$$

pp reference: interpolation of LHCb measurements at 2.76, 7, 8 and 13 TeV

Forward rapidity: suppression for both states, compatible with nPDFs

Backward rapidity: $\Upsilon(2S)$ more suppressed than $\Upsilon(1S)$, consistent with nPDFs+comovers calculation

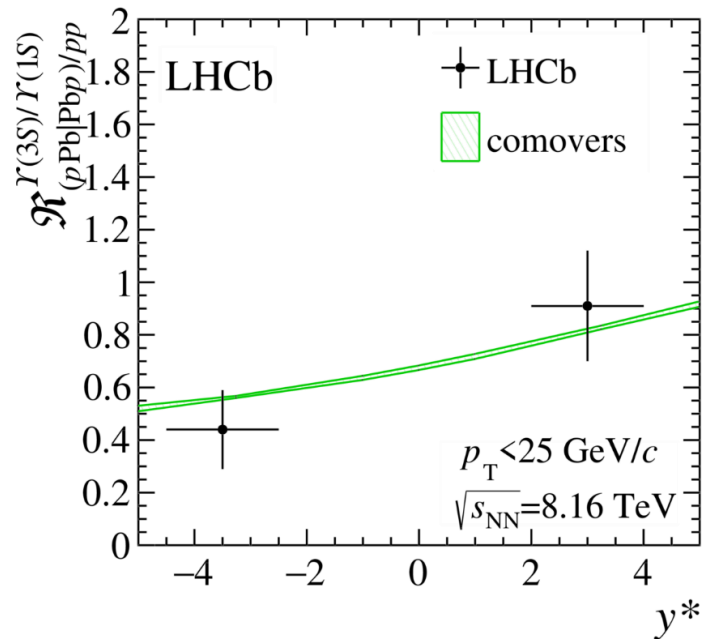
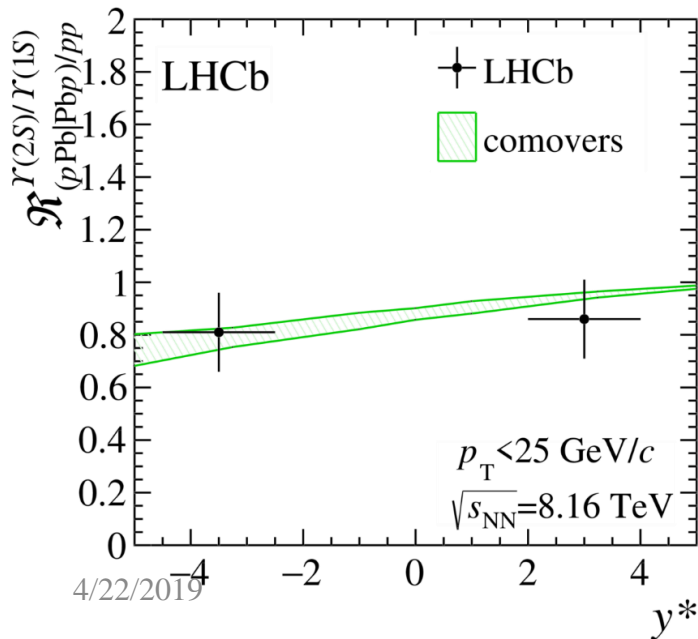


Double ratio

$$\mathcal{R}_{(pPb|Pbp)/pp}^{\Upsilon(nS)/\Upsilon(1S)} = \frac{R(\Upsilon(nS))_{pPb|Pbp}}{R(\Upsilon(nS))_{pp}}$$

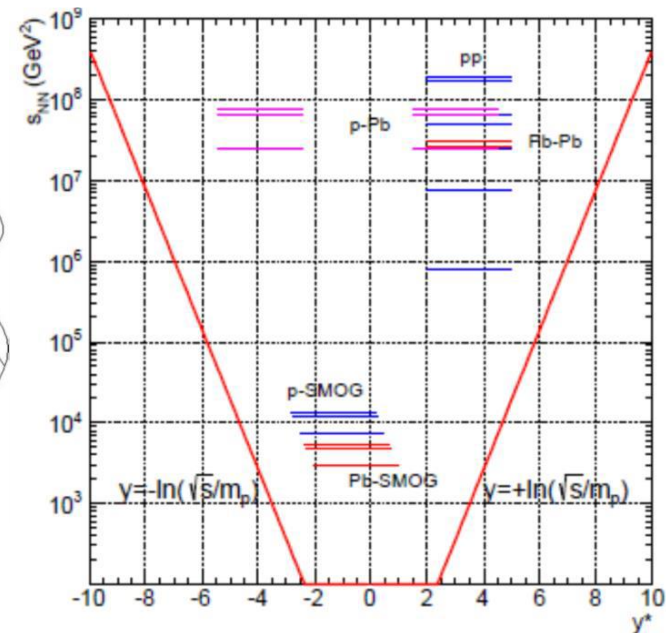
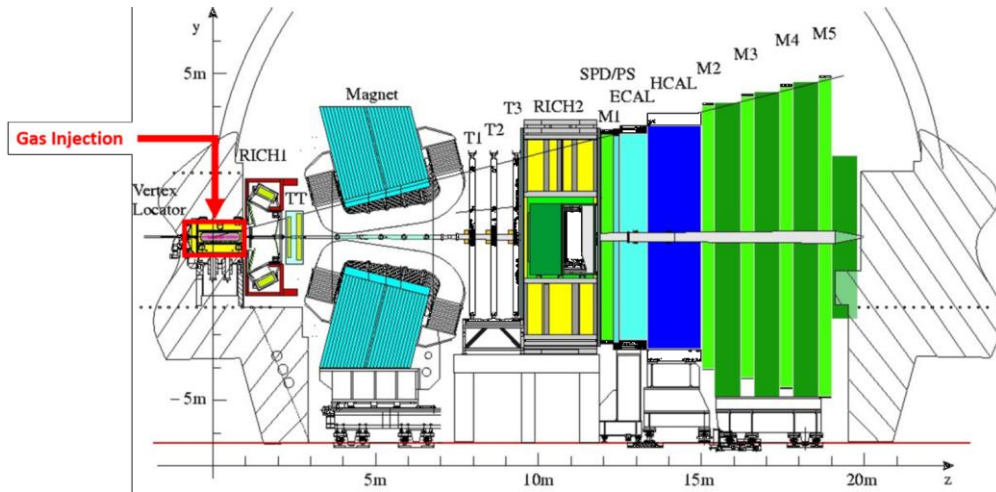
- Double ratio of $\Upsilon(nS)/\Upsilon(1S)$ in pPb and pp
- Sequential suppression also observed in pPb
- Suggests final state effects...
- Agrees with predictions of “comovers” model

$$R(\Upsilon(nS)) = \frac{[d^2\sigma/dp_T dy^*](\Upsilon(nS))}{[d^2\sigma/dp_T dy^*](\Upsilon(1S))}$$



Fixed target physics

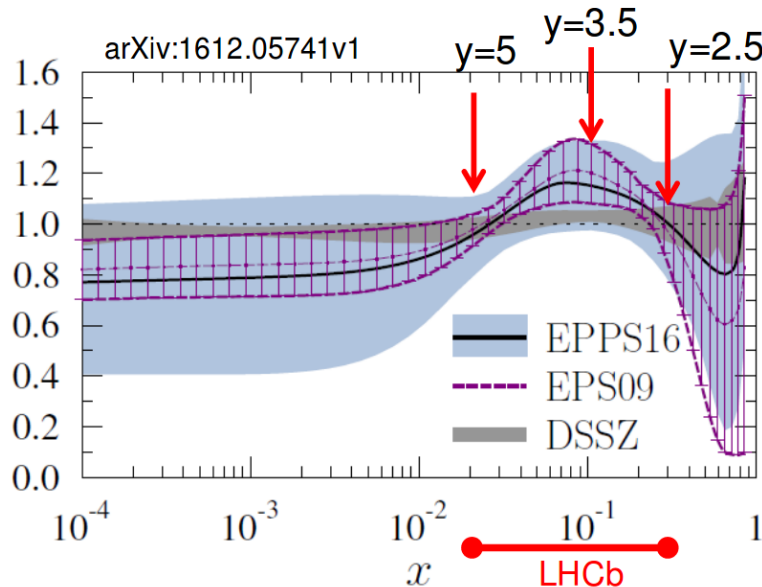
- LHCb: only experiment at the LHC can operate in fixed-target mode
- The System for Measuring Overlap with Gas (SMOG) allows a small amount of noble gas injection inside the LHC beam close to the interaction point
- Allows p -gas and ion-gas collisions
- $\sqrt{s_{NN}}$ region between 20 GeV (SPS) and 200 GeV (RHIC)
- Access nPDF anti-shadowing region and intrinsic charm content in the nucleon



Fixed target physics

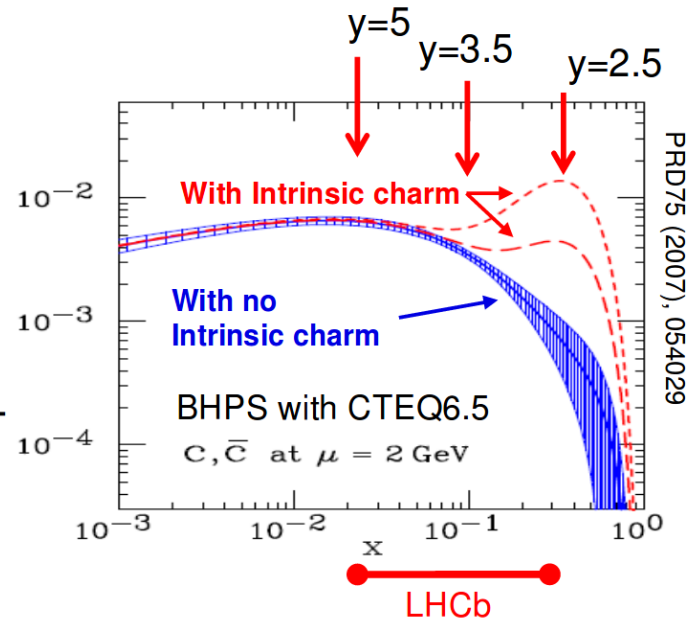
- LHCb: only experiment at the LHC can operate in fixed-target mode
- The System for Measuring Overlap with Gas (SMOG) allows a small amount of noble gas injection inside the LHC beam close to the interaction point
- Allows p -gas and ion-gas collisions
- $\sqrt{s_{NN}}$ region between 20 GeV (SPS) and 200 GeV (RHIC)
- Access nPDF anti-shadowing region and intrinsic charm content in the nucleon

PDF in a Pb nucleus/PDF in a single nucleon



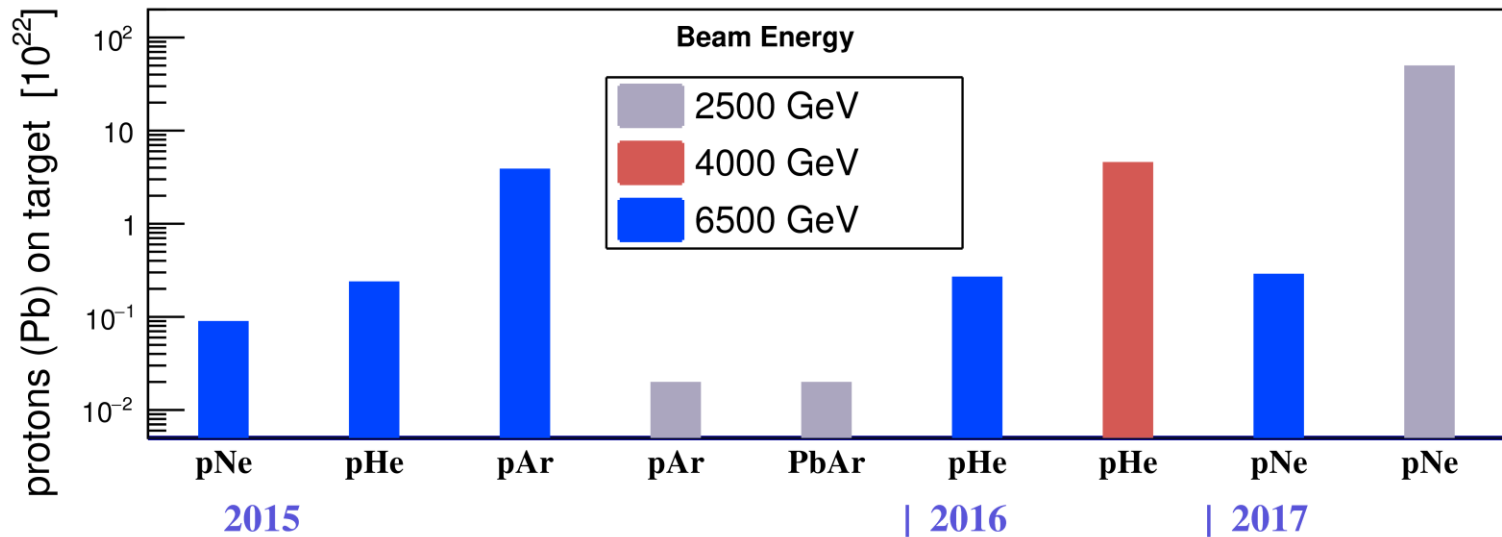
Bjorken- x = fraction of the nucleon momentum carried by a parton

Charm quark distributions



Data samples:

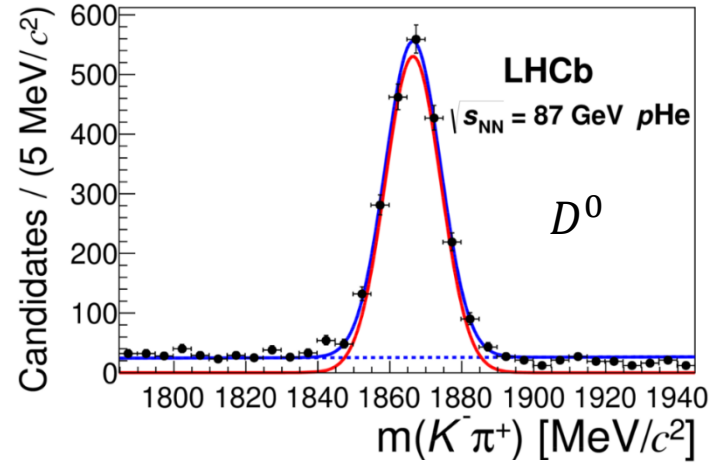
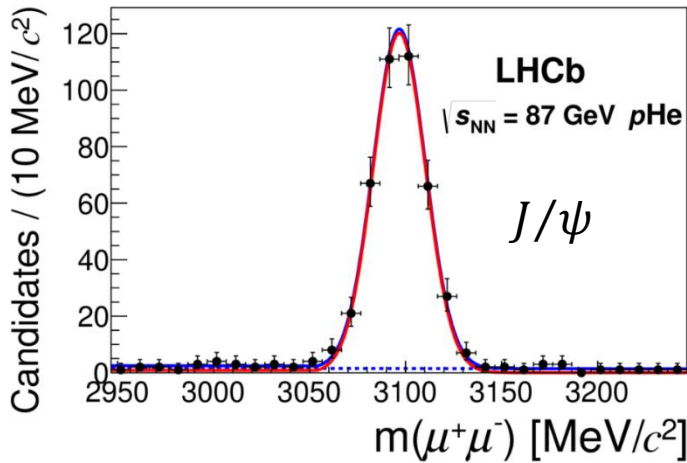
- $p\text{Ar}$ at $\sqrt{s_{NN}} = 110.4\text{GeV}$ (2015)
 - $\sim 4 \times 10^{22}$ Protons On Target
- $p\text{Ne}$ at $\sqrt{s_{NN}} = 86.6\text{GeV}$ (2016)
 - $\mathcal{L}_{p\text{Ne}} = 7.6 \pm 0.5\text{nb}^{-1}$
- $p\text{Ne}$ at $\sqrt{s_{NN}} = 110\text{GeV}$ (2016)
 - $\mathcal{L}_{p\text{Ne}} \sim 0.5\text{nb}^{-1}$



Charm production in fixed-target pN collision

Phys. Rev. Lett. 122 (2019) 132002

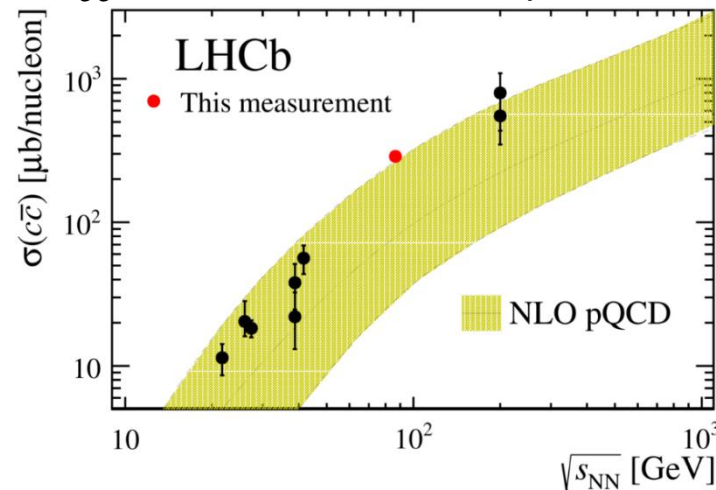
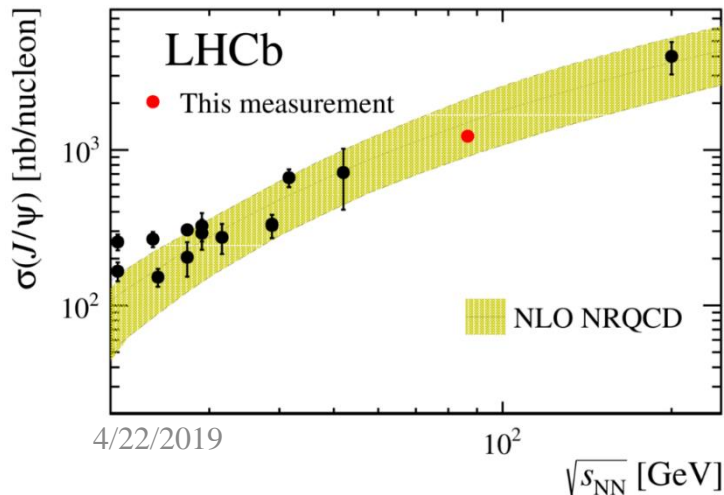
- J/ψ and D^0 inclusive cross-section in pNe collisions at 86.6 GeV
- First determination of $c\bar{c}$ cross-section at this energy scale



$$\sigma_{J/\psi} = 1225.6 \pm 100.7 \text{ nb/nucleon}$$

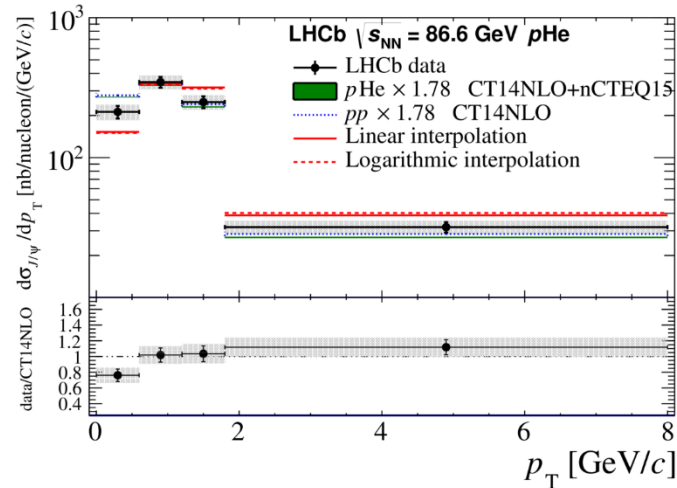
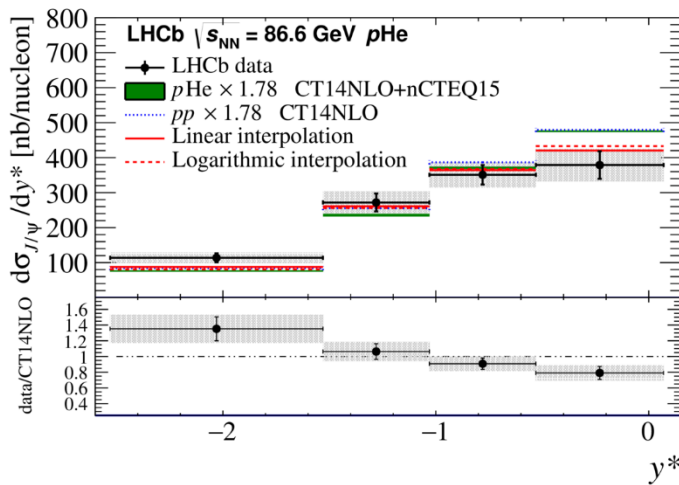
$$\sigma_{D^0} = 156.0 \pm 13.1 \text{ } \mu\text{b/nucleon}$$

$$\sigma_{c\bar{c}} = 288 \pm 24.2 \pm 6.9 \text{ } \mu\text{b/nucleon}$$

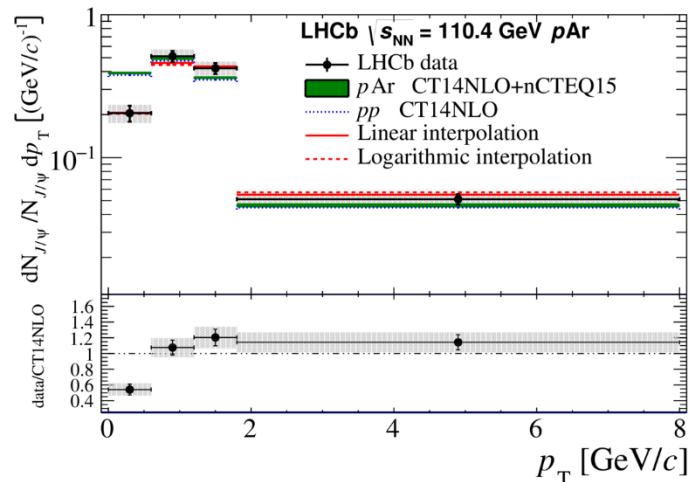
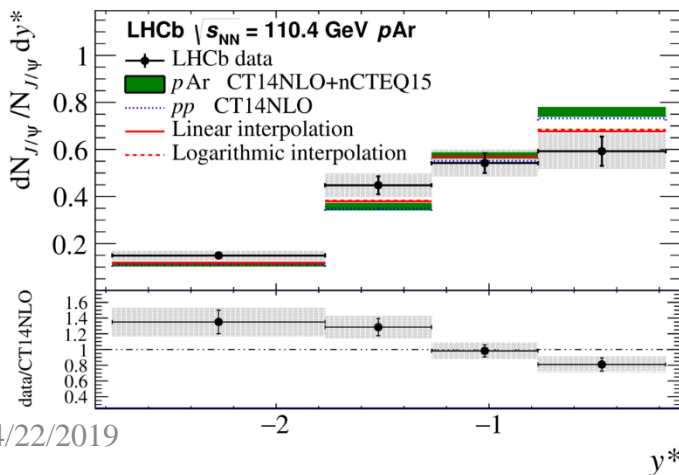


J/ψ production in fixed-target pN collision

- Differential cross-section (pNe @ 86.6 GeV)
- Differential yields (pAr @ 110.4 GeV)
- Helac-Onia underestimate the J/ψ cross-section by a factor of 1.78
- Reasonable agreement in rapidity shape



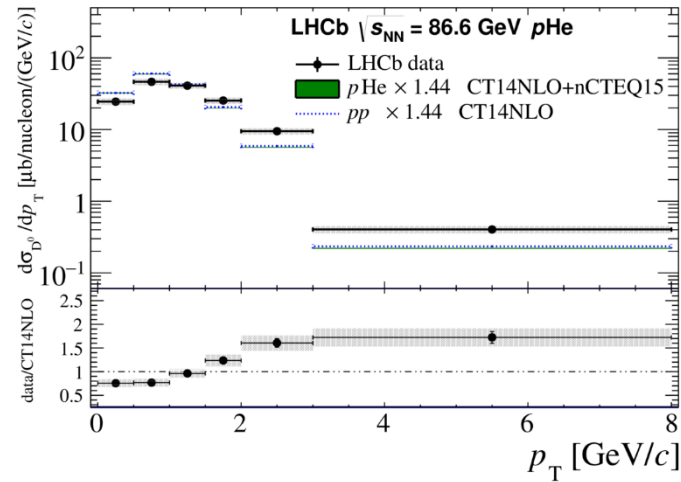
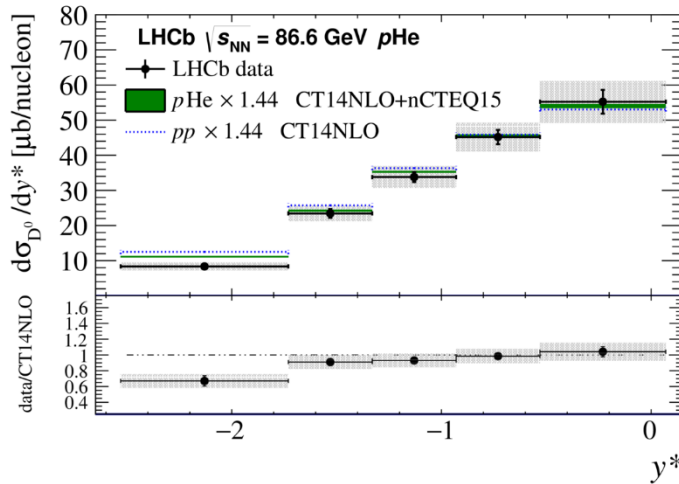
pNe
@ 86.6 GeV



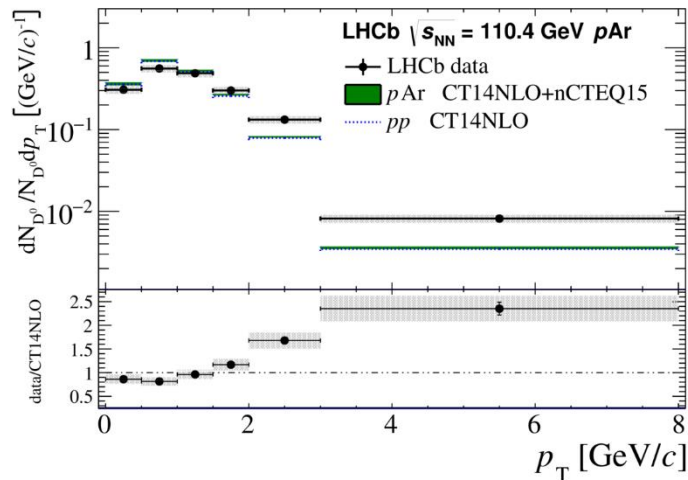
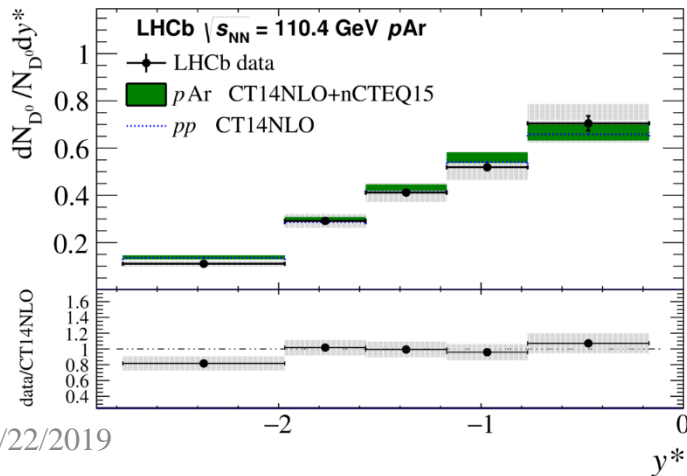
pAr
@ 110.4 GeV

D^0 production in fixed-target pN collision

- Differential cross-section (pNe @ 86.6 GeV)
- Differential yields (pAr @ 110.4 GeV)
- Helac-Onia underestimate the D^0 x-section by a factor of 1.44
- Reasonable agreement in rapidity shape



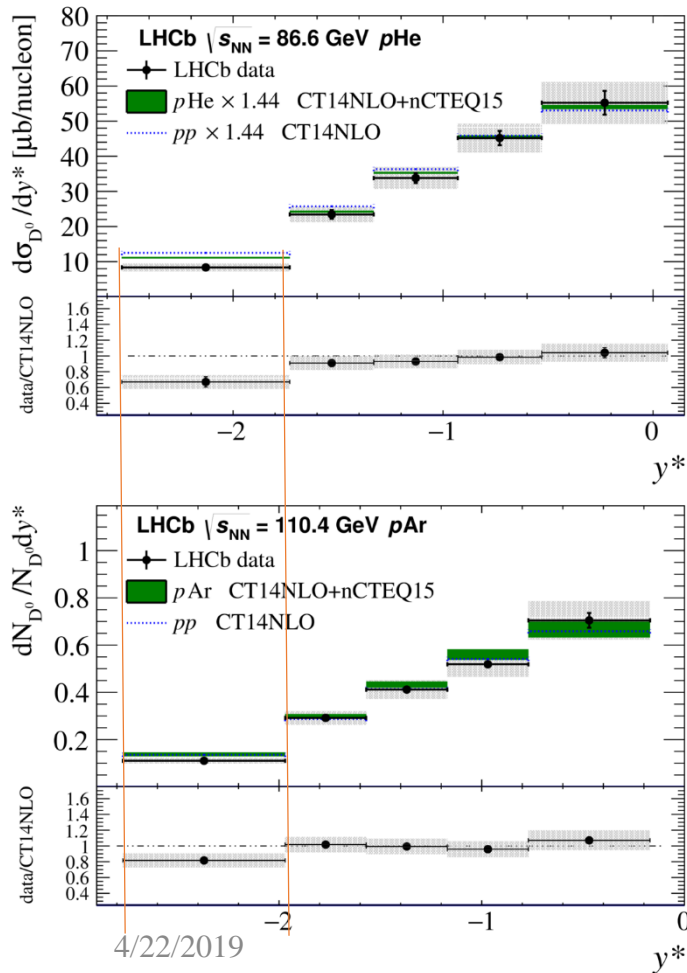
pNe
@ 86.6 GeV



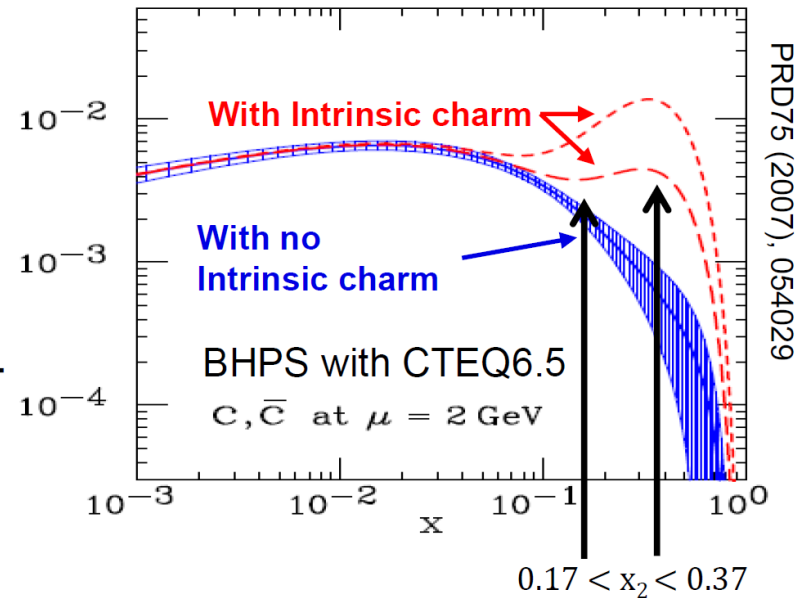
pAr
@ 110.4 GeV

Charm production in fixed-target pN collision

- $-2.53 < y^* < -1.73 \rightarrow 0.17 < x < 0.37$
- Little evidence of intrinsic charm observed

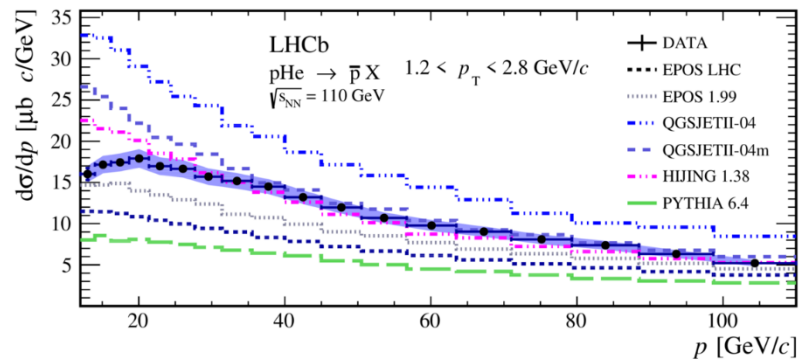
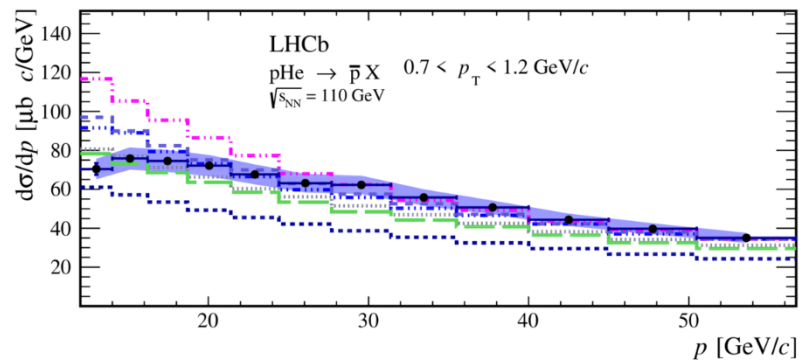
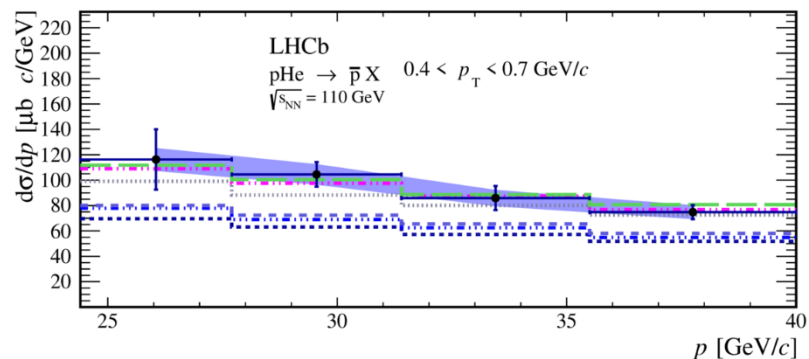
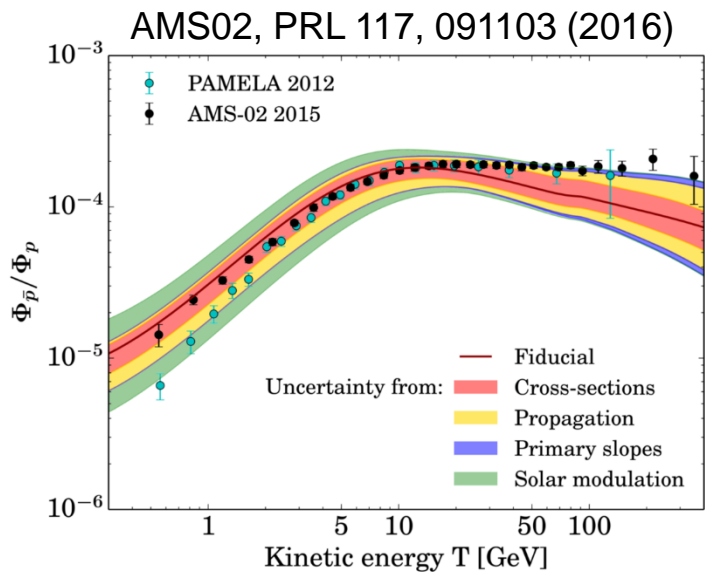


Charm quark distributions



$$x \approx \frac{2m_c}{\sqrt{s_{NN}}} \exp(-y^*)$$

\bar{p} production in p He collisions



- AMS-2: possible anti-proton excess at high energies
- \bar{p}/p ratio predictions limited by uncertainties on \bar{p} production cross-sections, particularly for p -He
- Prompt production at $\sqrt{s_{NN}} = 110 \text{ GeV}$
- First measurement of \bar{p} production in p Ne
- Uncertainty smaller than the spread of models

Conclusion

- Recent results with heavy ions at LHCb
 - Heavy quarkonia in $p\text{Pb}$: J/ψ and $\Upsilon(nS)$
 - Fixed-target mode: charm and antiproton
- For the future
 - Analyses of other quarkonia using the $p\text{Pb}$ dataset
 - 2018 PbPb dataset (20 times larger than 2015)
 - Upgrade for Run3/4
 - Upgrade of SMOG system for Run3
 - More gases (H_2 , deuteron...)
 - Density of the target gas increase \rightarrow luminosity increase up to a factor of 100